Production of hydrogen peroxide in the atmosphere of a Snowball Earth and the origin of oxygenic photosynthesis

Mao-Chang Liang*†‡, Hyman Hartman§, Robert E. Kopp*, Joseph L. Kirschvink*, and Yuk L. Yung*

*Division of Geological and Planetary Sciences, California Institute of Technology, 1200 East California Boulevard, Pasadena, CA 91125; §Center for Biomedical Engineering, Massachusetts Institute of Technology, 31 Ames Street, Cambridge, MA 02139-4307; and †Research Center for Environmental Changes, Academia Sinica, 128 Academia Road, Section 2, Nankang, Taipei 115, Taiwan

During Proterozoic time, Earth experienced two intervals with one or more episodes of low-latitude glaciation, which are probable ''Snowball Earth'' events. Although the severity of the historical glaciations is debated, theoretical ''hard Snowball'' conditions are associated with the nearly complete shutdown of the hydrological cycle. We show here that, during such long and severe glacial intervals, a weak hydrological cycle coupled with photochemical reactions involving water vapor would give rise to the sustained production of hydrogen peroxide. The photochemical production of hydrogen peroxide has been proposed previously as the primary mechanism for oxidizing the surface of Mars. During a Snowball, hydrogen peroxide could be stored in the ice; it would then be released directly into the ocean and the atmosphere upon melting and could mediate global oxidation events in the aftermath of the Snowball, such as that recorded in the Fe and Mn oxides of the Kalahari Manganese Field, deposited after the Paleoproterozoic low-latitude Makganyene glaciation. Low levels of peroxides and molecular oxygen generated during Archean and earliest Proterozoic non-Snowball glacial intervals could have driven the evolution of oxygen-mediating and -using enzymes and thereby paved the way for the eventual appearance of oxygenic photosynthesis.

atmospheric processes | Paleoproterozoic | photochemistry

Hydrogen peroxide provides a powerful oxidant in anoxic environments. The recent discovery of H_2O_2 in the atmosphere of Mars (1, 2) supports the hypothesis that oxidation of iron by photochemically generated H_2O_2 over the past 4 billion years may have yielded the present oxidized Martian surface (3). The cold, dry, and low-oxygen (≈ 7 μbar) Martian atmosphere concentrates H_2O_2 production near the surface (4, 5). Hydrogen peroxide can be preserved readily in ice, because H_2O_2 has a slightly lower freezing point ($-1°C$) than H_2O; a concentration of H_2O_2 as high as 0.13% is observed on the surface of the Galilean satellite Europa (6). The closest analog in Earth history for the cold, dry, low-oxygen conditions of Mars and Europa may have occurred during the proposed Paleoproterozoic Snowball Earth event (7, 8) and perhaps during one or both of the proposed Neoproterozoic Snowball Earth events (9, 10).

Although there have been many glacial events recorded in the history of the Earth (9–11), two major periods of low-latitude glaciation in the Proterozoic appear correlated with significant changes in the evolution of life (8, 12–14) and atmospheric oxygen level (15–19). The Paleoproterozoic Makganyene glaciation occurred approximately between 2.3 and 2.2 Ga, and at least two other low-latitude glaciations occurred during the Cryogenian period, between ≈ 740 and 630 Ma (9, 10, 20). The severity of these ''Snowball Earth'' events is debated, but the low latitude of the glaciations indicates that, at least on the continents, ice extended to the equator, average global temperatures were likely well below freezing, and the hydrological cycle was much diminished (21, 22). The rock record indicates that the atmosphere and ocean were oxygen-poor until shortly before the onset of the Paleoproterozoic Snowball at ≈ 2.3 Ga (15–19), and the weakening of the biosphere and hydrological cycle would likely have decreased atmospheric oxygen levels during the event. Here we adopt a photochemical model similar to the one that Nair et al. (4) successfully applied to the Martian atmosphere to investigate the production and deposition of H_2O_2 during low-oxygen Snowball Earth conditions.

We examined atmospheric photochemistry during the Paleoproterozoic Snowball Earth event, as well as the impact of earlier glaciations on the evolution of cellular life. Assuming the Paleoproterozoic Makganyene glaciation was a ''hard Snowball,'' it led to an environment similar to that on Mars and icy satellites, where H_2O_2 could be produced and preserved in ice. During the deglaciation, the deposited H_2O_2 would have been released into the oceans and atmosphere, as occurs during the spring and summer in Greenland and at the South Pole (23, 24). On a low-oxygen planet, the H_2O_2 could have provided an important source of oxidants for driving the evolution of oxygen-mediating and -using enzymes.

Atmospheric Chemical Models

We performed a one-dimensional diurnally averaged simulation of the chemical processes in the atmosphere of a Snowball Earth. Our model calculates the profiles of O, $O(^1D)$, O_2, O_3, H, H_2, OH, HO_2, H_2O_2, CO, CO_2, HCO, and H_2CO by solving the mass continuity equation $(\partial n_i/\partial t) + (\partial \varphi_i/\partial z) = P_i - L_i$, where n_i is the number density for species i, φ_i is the vertical flux, P_i is the chemical production rate, and L_i is the chemical loss rate, all evaluated at time t and altitude z. P_i and L_i are calculated based on the chemical schemes published in the literature (4, 25–27). The vertical flux is given by

$$\varphi_i = -\frac{\partial n_i}{\partial z}(D_i + K_{zz}) - n_i\left(\frac{D_i}{H_i} + \frac{K_{zz}}{H_{atm}}\right)$$
$$- n_i\frac{\partial T}{\partial z}\left[\frac{(1 + \alpha_i)D_i + K_{zz}}{T}\right], \quad [1]$$

where D_i is the species' molecular diffusion, H_i is the species' scale height, H_{atm} is the atmospheric scale height, α_i is the thermal diffusion parameter, and T is the temperature. The vertical eddy mixing coefficient K_{zz} in this work is set to be 2×10^5 $cm^2 \cdot s^{-1}$, which is close to the present-day value near the surface (25). With this K_{zz}, the vertical mixing time is on the order of 10^6 s, a value much longer than the lifetime of H_2O_2 of

Fig. 1. Profiles of H_2O (dotted line), H_2O_2 (solid line), O_2 (dash-dotted line), H_2 (triple dot-dashed line), CO (long-dashed line), and CO_2 (dashed line) calculated with the reference model, in which surface temperature is 240 K, temperature gradient is -10 K km^{-1}, and constant temperature is 150 K above the tropopause (≈ 10 km). The values are shown for the model calculation at one instance at the end of the Snowball Earth. The downward and escape fluxes of H_2O_2 and H_2 are $\approx 5 \times 10^8$ and 10^{10} molecules cm^{-2}·s^{-1}, respectively. The mixing ratio of H_2O above the tropopause is set equal to that at the tropopause.

Fig. 2. Profiles of H (solid line), O (dotted line), O_3 (dashed line), HCO (dash-dotted line), and H_2CO (triple dot-dashed line) under the same conditions as Fig. 1.

$\approx 10^4$ s in the atmosphere. We therefore expect that K_{zz} plays a minor role in the vertical profile of H_2O_2.

Because of model limitations, we assume the surface pressure is 1 bar over the course of model time. We fix the H_2O profile at that determined by its saturation pressure in the atmosphere; we vary the profile by modifying the surface temperature. For the temperature profile, the surface temperature is taken to be 240 K, with a vertical temperature gradient of -10 K·km^{-1} (dry-adiabatic lapse rate) and a constant temperature of 150 K in regions where the extrapolation of the temperature with the assumed gradient yields values <150 K; this is quoted as the reference model. We also assume a present-day solar UV spectrum. Initially, the atmosphere contains N_2 and H_2O only. The model starts with an upward H_2 and CO_2 flux of 10^{10} molecules cm^{-2}·s^{-1}, which are close to the current volcanic outgassing rates (13). Species other than H_2, H_2O, and H_2O_2 are impermeable at the boundary. We allow H_2 to escape to space hydrodynamically when the conditions of Tian *et al.* (28) are met, although the strength of hydrodynamic escape in this paleoatmosphere remains inconclusive (29). The model results with both higher and lower levels of hydrogen escape are also presented. With the present-day solar spectrum, hydrodynamic escape happens when the homopause (≈ 65 km) mixing ratio of H_2 is >0.05. To a first-order approximation, we assume that H_2 escape with a flux of 10^{10} molecules cm^{-2}·s^{-1} is initiated when the H_2 mixing ratio is >0.1 and that it remains at this level as long as the ratio is >0.05. We let the model run for the entire lifetime of the Snowball (see below). Vertical profiles of species important to this study are summarized in Fig. 1; some other profiles are presented in Fig. 2. Note that formaldehyde, which can be preserved on the surface by precipitation (27), is not produced in large amounts, so the deposition of H_2 by burying H_2CO is insignificant.

Current thinking suggests that deglaciation would proceed from build-up of greenhouse gases such as CO_2 due to persistent volcanic activity uncompensated by silicate weathering. As ice cover and low temperatures would have greatly hindered silicate weathering, atmospheric accumulation of greenhouse gases, particularly CO_2, would have eventually allowed temperatures to

rise above freezing (30). In Neoproterozoic time, over the likely 12-million-year lifetime of the Snowball event (20), atmospheric CO_2 could have reached a level of 0.2 bar at the present-day outgassing rate of $\approx 10^{10}$ molecules cm^{-2}·s^{-1}. Although it has recently been noted that greenhouse warming caused directly by CO_2 at a level as high as 0.2 bar may not have been sufficient to initiate the deglaciation of Neoproterozoic Snowballs (30, 31), in our model we still follow typical suggestions to estimate the duration of the Paleoproterozoic Snowball event. Assuming 0.2 bar CO_2 was actually required to start the Neoproterozoic deglaciations, the lower solar constant in the Paleoproterozoic (85% of modern insolation, rather than 96%) implies that triggering the end of a Paleoproterozoic Snowball would have required ≈ 0.6 bar CO_2. At present degassing rates, such an amount would have taken ≈ 35 million years to build up (32).

Hydrogen Peroxide Deposition

Hydrogen peroxide can be deposited on ice by diffusional contact. This deposition rate is limited by the lifetime of H_2O_2 against photolysis in the atmosphere (≈ 6 h), equivalent to a traveling distance of <1 km for a diffusion coefficient of 2×10^5 cm^{-2}·s^{-1}. The diffusional deposition of H_2O_2 is also sensitive to the H_2/O_2 ratio (Fig. 3). The abundance of H_2 reflects the strength of hydrogen escape to space. With a ratio of ≈ 2 the deposition rate is as high as 10^{10} molecules cm^{-2}·s^{-1}. For ratios >5, the rates are suppressed by a factor of >10. The accumulation of H_2 in the atmosphere would soon stop the diffusional deposition of H_2O_2 if the replenishment of O_2 were insufficient to support an O_2 abundance as high as that in Fig. 1, because of the reaction $2H_2 + O_2 \rightarrow 2H_2O$. We find that the continuous accumulation and photolysis of CO_2 in the atmosphere can maintain such a level of O_2 ($2CO_2 \rightarrow 2CO + O_2$) via well known HOx chemistry (26). Consequently, CO is in high abundance (Fig. 1). Because the photolytic processes of CO_2 and H_2O are in similar wavelength ranges, by the end of the Snowball CO_2 becomes a major UV absorber and H_2O photolysis is less significant. In this standard model, the deposition rate of H_2O_2 by diffusion is 3×10^8 molecules cm^{-2}·s^{-1}.

For the H_2O_2 precipitation rate, we follow the method developed for modern glacial environments (23, 24) to estimate a concentration of H_2O_2 in snowfall of ≈ 20 μM. Incorporating the estimated H_2O_2 diffusional flux to surface ice and assuming a hydrological cycle of f mm·yr^{-1}, this standard model yields a volume mixing ratio of H_2O_2 in the snow/ice as high as $\approx 3 \times 10^{-6}(1/f)$ if $f < 10$, and as low as $\approx 5 \times 10^{-7}$ if $f > 10$. Enhancing
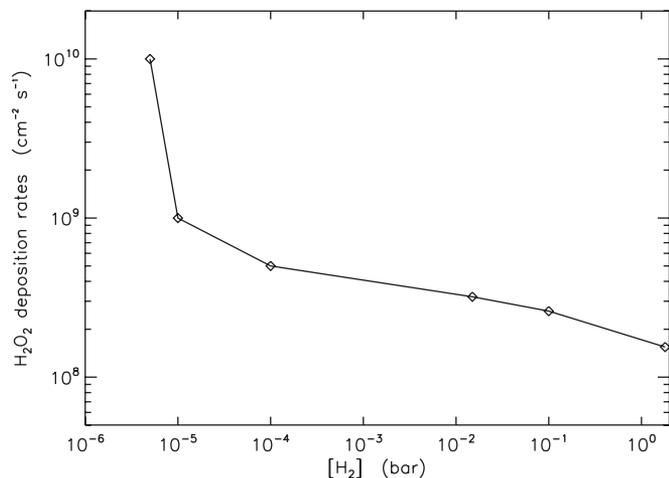
Fig. 3. Sensitivity of surface H_2 abundance, obtained by varying the strength of hydrogen hydrodynamic escape, on the deposition rate of H_2O_2 by diffusion. The abundance of O_2 as high as that in Fig. 1 is maintained by CO_2 photolysis (see text). The rightmost point is calculated by assuming that H_2 escape vanishes. For the diffusion-limit hydrogen escape case, the surface H_2 mixing ratio is $\approx 5 \times 10^{-4}$ and the H_2O_2 deposition rate is $\approx 4 \times 10^8$ molecules $cm^{-2} \cdot s^{-1}$.

Fig. 4. Sensitivity of surface temperature on the deposition rate of H_2O_2 by diffusion. The vertical profiles of major compounds (e.g., H_2, O_2, CO, and CO_2) are similar to those in Figs. 1 and 2.

the hydrological cycle will always enhance the rainout rate of H_2O_2 as well as the concentration of H_2O_2 in H_2O ice, by analogy with evaporation processes in H_2O_2-H_2O solution, which enhance the concentration of H_2O_2 in the solution (33). This further concentration of H_2O_2 in the ice depends on the partitioning of H_2O_2 and H_2O in vapor during evaporation (knowledge of which is not available for low-temperature conditions), the lifetime of ice sheet (34), and the strength of hydrological cycles or precipitation/evaporation rates (31, 34). A one-dimensional model of the dynamics of ice on a Snowball Earth has been published (34).

Changing surface temperature will also modify the calculated deposition rate of H_2O_2 by diffusional contact. Reducing surface temperature will correspondingly reduce the atmospheric H_2O vapor abundance and hence move the oxidation line (the region of the atmosphere where H_2O_2 is mostly produced) closer to the surface. This shift will enhance diffusional H_2O_2 deposition, because the lifetime of H_2O_2 is short compared with vertical transport time (10^4 vs. 10^6 s; see above). The results of tests of sensitivity to changes of surface temperature are summarized in Fig. 4. In general, reducing surface temperatures will enhance the deposition rate by diffusion but will reduce the rainout rate.

Direct rainout from H_2O_2 nucleation in the region between ≈ 10 and 20 km is not included in the current model; the partial vapor pressure of H_2O_2 is $\approx 5 \times 10^{-8}$ mbar, which is greater than the saturation pressure (33) of $\approx 10^{-9}$ mbar at 150 K. If this amount of H_2O_2 is removed by rainout, an additional precipitation rate of $\approx 10^{10}$ molecules $cm^{-2} \cdot s^{-1}$ (equal to the production rate in this region) is imposed, yielding the total volume mixing ratio of H_2O_2 in the ice as high as $10^{-4}(1/f)$. Note that the total production rate of H_2O_2 by gas-phase chemistry is $\approx 10^{11}$ molecules $cm^{-2} \cdot s^{-1}$, which provides an upper limit to the rate of H_2O_2 deposition by diffusion and precipitation.

We stress that the calculated concentration of H_2O_2 in the snow/ice is a lower limit. With the present-day solar spectrum, the maximum photolysis rate of H_2O is $\approx 10^{12}$ molecules $cm^{-2} \cdot s^{-1}$. If UV photons directly irradiated the snow/ice, H_2O_2 could be produced and preserved readily in the ice. For example, the production rate of H_2O_2 in Antarctic seawater samples by direct sun light irradiation has been shown to approach this maximum H_2O photolysis rate (35). Recently, it has also been
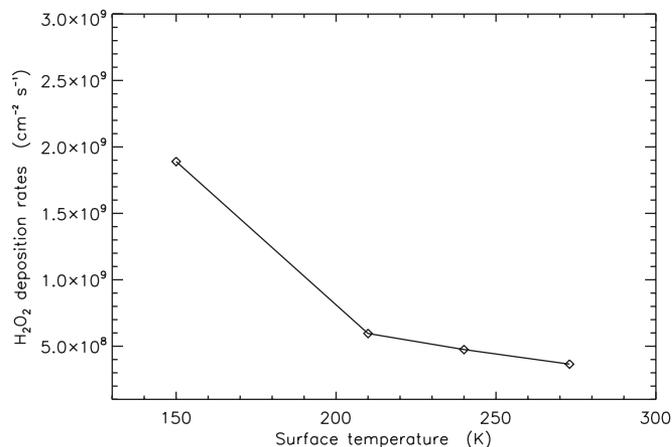
shown that H_2O_2 at the surface is enhanced when stratospheric ozone is depleted (36), as in an anaerobic atmosphere. This mechanism of depositing H_2O_2 would be insensitive to the abundance of atmospheric H_2.

In summary, we find that the volume mixing ratio of H_2O_2 in the ice falls between 5×10^{-7} and $10^{-4}(1/f)$. The lower limit represents the regions where water cycles (precipitation/evaporation and ice melting) are active, as might occur at midday, in the summer, and in low-latitude regions. The upper limit can be achieved where water cycles are weak, such as in mid to high latitudes of the winter hemisphere (31). For example, at low latitudes of the summer hemisphere, the water precipitation could be as high as 45 $cm \cdot yr^{-1}$ (31), resulting in the mixing ratio of H_2O_2 in the ice $\approx 5 \times 10^{-7}$. At winter hemisphere mid to high latitudes, pure H_2O_2 rainout is possible, because of low water cycles (31). Coupled with sea ice flow (34), a high level of H_2O_2 ice formed at mid to high latitudes can be transported to a lower latitude. Consequently, high-concentration H_2O_2 ice is available globally on the Snowball Earth. (A volume mixing ratio of H_2O_2 of 10^{-3} stored in 1-km-thick ice could disproportionate to form the equivalent to 0.1 bar of O_2.) We note that the above estimation is simply based on snowfalls and dry deposition. The direct freezing of sea water could affect the concentration of H_2O_2 in the frozen ice; however, this process is sensitive to the strength of dynamical mixing in sea water. High concentrations of H_2O_2 in the ice may significantly suppress hydrological cycles. Future work is needed to resolve the aforementioned uncertainties.

Biological Implications

Even when the concentration of H_2O_2 in snow and ice is as low as that in modern polar regions, the release of H_2O_2 into the ocean upon melting could provide an environmental oxidant that would threaten organisms living nearby. Hydrogen peroxide in the presence of ferrous ion produces the hydroxyl radical (and ferryl iron), which is lethal to the cell (37). The Mn-based enzyme catalase, which catalyzes the reaction $2H_2O_2 \rightarrow 2H_2O + O_2$ (38, 39), and the superoxide dismutase enzymes, which neutralize O_2^-, protect the cell against the effects of hydrogen peroxide and the hydroxyl radical. These enzymes likely evolved before the evolution of oxygenic photosynthesis and hence protected the first oxygen-producing phototroph (40), perhaps in response to an environmental peroxide challenge. Blankenship and Hartman (41) further suggested that H_2O_2 played a crucial role in the origin and evolution of oxygenic photosynthesis because it is capable of being both a powerful oxidant and a

reductant and because the oxidation of H_2O_2 to O_2 is fully within the oxidative capabilities of reaction centers from existing anoxygenic photosynthetic bacteria (41). The Huronian glaciations at ≈2.4–2.3 Ga (8), the Pongola glaciations at ≈2.9 Ga (42), and perhaps unrecognized earlier glacial episodes might thus have spurred their development of both oxygen tolerance and oxygenic photosynthesis (40, 41), as well as stimulated the evolution of diverse oxidase and peroxidase enzymes that are now critical for aerobic metabolism.

Kopp et al. (8) proposed that the severity of the Makganyene Snowball Earth event was caused by the evolution of efficient oxygenic photosynthesis during the short interval between the Huronian glaciations and the Makganyene glaciation, and that photosynthetic oxygen production at the onset of the Makganyene glaciation triggered a collapse of the methane greenhouse. The evolution of oxygen tolerance in response to peroxide build-up during the Huronian glaciations could have paved the way for this evolutionary step.

Only a planetary glaciation like a Snowball Earth event, however, would be likely to produce enough H_2O_2 to leave a global fingerprint. During a Snowball, as ocean waters cycled through hydrothermal vents, the concentration of metals like Fe^{2+} and Mn^{2+} would have built up to high levels. After the Snowball, as recorded in the Kalahari Manganese Field (7) and in lesser Neoproterozoic manganese deposits like those of the Urucum district (43), iron and manganese would have been oxidized by oxygen and precipitated out of solution. After the Neoproterozoic Snowballs the main source of oxygen was likely atmospheric, but after the Makganyene Snowball atmospheric oxygen was still fairly low. The oxygen source for the Kalahari Manganese Field was probably a combination of a post-Snowball cyanobacterial bloom (7) and disproportionation of H_2O_2.

Fennel et al. (44) recognized recently that nitrate limitation is a critical problem in the transition from an anaerobic to an aerobic environment, such as presumably occurred around 2.3 Ga at the "Great Oxygenation Event." Starting from an anaerobic environment, increasing oxidation removes metal cofactors critical for the function of the nitrogenase enzyme, as well as enabling aerobic denitrification. In turn, nitrogen limitation acts to constrict productivity, keeping the global production of oxygen by the cyanobacteria at levels below those needed to transition into the modern, oxygen-dominated stable environment in which abundant nitrate is biologically available. Fennel et al. (44) offer no clear explanation of how this "biogeochemical bottleneck" barrier between the anaerobic and aerobic stable states of the planetary ecosystem could be crossed. We suggest tentatively that the post-Makganyene snowball "burp" of peroxide (which in some model scenarios could be on the order of 1 bar) might have pushed the global environment over this nitrate limitation barrier by throwing the surface ocean into the oxic, nitrate-rich realm. More sophisticated modeling is necessary to test this idea.

We have demonstrated here that the generation of H_2O_2 through photolytic processes involving H_2O is possible in the oxygen-poor early atmosphere of the Archean and early Paleoproterozoic (45, 46). Large amounts of hydrogen peroxide can be preserved only under special conditions, such as during an intense glaciation. Because of the short atmospheric lifetime of H_2O_2 against UV photolysis, build-up of large amounts requires H_2O_2 production close to the ground (hence, under low-O_2 conditions), as well as a mechanism to trap it in the ice to store and concentrate it. During an intense glaciation, particularly a Snowball event, the H_2O_2 deposition rate may have been enhanced greatly, as we discuss above, although our model is extremely simple and excludes many important considerations. A coupled chemistry (gas-phase and solid-state) and dynamics (climate and ice-sheet) model is needed to quantify our calculation in detail and to provide a more accurate and quantitative estimation of the deposition of hydrogen peroxide during glaciations in anaerobic atmospheres as well as Snowball Earth events.

1. Clancy RT, Sandor BJ, Moriarty-Schieven GH (2004) *Icarus* 168:116–121.
2. Encrenaz T, Bezard B, Greathouse TK, Richter MJ, Lacy JH, Atreya SK, Wong AS, Lebonnois S, Lefevre F, Forget F (2004) *Icarus* 170:424–429.
3. Hunten DM (1979) *J Mol Evol* 14:71–78.
4. Nair H, Allen M, Anbar AD, Yung YL, Clancy RT (1994) *Icarus* 111:124–150.
5. Yung YL, DeMore WB (1999) *Photochemistry of Planetary Atmospheres* (Oxford Univ Press, New York).
6. Carlson RW, Anderson MS, Johnson RE, Smythe WD, Hendrix AR, Barth CA, Soderblom LA, Hansen GB, McCord TB, Dalton JB, *et al.* (1999) *Science* 283:2062–2064.
7. Kirschvink JL, Gaidos EJ, Bertani LE, Beukes NJ, Gutzmer J, Maepa LN, Steinberger RE (2000) *Proc Natl Acad Sci USA* 97:1400–1405.
8. Kopp RE, Kirschvink JL, Hilburn IA, Nash CZ (2005) *Proc Natl Acad Sci USA* 102:11131–11136.
9. Chumakov NM, Elston DP (1989) *Episodes* 12:115–119.
10. Hambrey MJ, Harland WB (1981) *Earth's Pre-Pleistocene Glacial Record* (Cambridge Univ Press, Cambridge, UK).
11. Young GM, von Brunn V, Gold DJC, Minter WEL (1998) *J Geol* 106:523–538.
12. Chen JY, Bottjer DJ, Oliveri P, Dornbos SQ, Gao F, Ruffins S, Chi HM, Li CW, Davidson EH (2004) *Science* 305:218–222.
13. Holland HD (2002) *Geochim Cosmochim Acta* 66:3811–3826.
14. Xiao SH, Zhang Y, Knoll AH (1998) *Nature* 391:553–558.
15. Bekker A, Holland HD, Wang PL, Rumble D, III, Stein HJ, Hannah JL, Coetzee LL, Beukes NJ (2004) *Nature* 427:117–120.
16. Farquhar J, Bao H, Thiemens M (2000) *Science* 289:756–758.
17. Karhu JA, Holland HD (1996) *Geology* 24:867–870.
18. Catling DC, Claire MW (2005) *Earth Planet Sci Lett* 237:1–20.
19. Canfield DE (2005) *Annu Rev Earth Planet Sci* 33:1–36.
20. Bodiselitsch B, Koeberl C, Master S, Reimold WU (2005) *Science* 308:239–242.
21. Hoffman PF, Schrag DP (2002) *Terra Nova* 14:129–155.
22. Kirschvink JL (1992) *The Proterozoic Biosphere: A Multidisciplinary Study* (Cambridge Univ Press, Cambridge, UK).
23. Hutterli MA, McConnell JR, Stewart RW, Jacobi HW, Bales RC (2001) *J Geophys Res Atmos* 106:15395–15404.
24. Hutterli MA, McConnell JR, Chen G, Bales RC, Davis DD, Lenschow DH (2004) *Atmos Environ* 38:5439–5450.
25. Allen M, Yung YL, Waters JW (1981) *J Geophys Res Space Phys* 86:3617–3627.
26. Liang MC, Lane BF, Pappalardo RT, Allen M, Yung YL (2005) *J Geophys Res Planets* 110, 10.1029/2004JE002322.
27. Pinto JP, Gladstone GR, Yung YL (1980) *Science* 210:183–184.
28. Tian F, Toon OB, Pavlov AA, Sterck HD (2005) *Science* 308:1014–1017.
29. Catling DC (2006) *Science* 311:38.
30. Pierrehumbert RT (2004) *Nature* 429:646–649.
31. Pierrehumbert RT (2005) *J Geophys Res Atmos* 110, 10.1029/2004JD005162.
32. Tajika E (2003) *Earth Planet Sci Lett* 214:443–453.
33. Manatt SL, Manatt MRR (2004) *Chem Eur J* 10:6540–6557.
34. Goodman JC, Pierrehumbert RT (2003) *J Geophys Res Oceans* 108, 10.1029/2002JC001471.
35. Abele D, Ferreyra GA, Schloss I (1999) *Antarctic Sci* 11:131–139.
36. Frey MM, Stewart RW, McConnell JR, Bales RC (2005) *J Geophys Res Atmos* 110, 10.1029/2005JD006110.
37. Touati D (2000) *Arch Biochem Biophys* 373:1–6.
38. Penner-Hahn JE (1992) *Manganese Redox Enzymes* (VCH, New York).
39. Stumm W, Morgan JJ (1996) *Aquatic Chemistry: Chemical Equilibria and Rates in Natural Waters* (Wiley, New York).
40. Schopf JW (1993) *Science* 260:640–646.
41. Blankenship RE, Hartman H (1998) *Trends Biochem Sci* 23:94–97.
42. Nhelko N (2004) in *Geology* (Rand Afrikaans Univ, Johannesburg), p 285.
43. Klein C, Ladeira EA (2004) *Econ Geol* 99:1233–1244.
44. Fennel K, Follows M, Falkowski PG (2005) *Am J Sci* 305:526–545.
45. McKay CP, Hartman H (1991) *Origins Life Evol Biosphere* 21:157–163.
46. Kasting JF, Holland HD, Pinto JP (1985) *J Geophys Res Atmos* 90:497–510.

ENVIRONMENTAL SCIENCES